Surface Stability of Polypropylene Compounds and Paint Adhesion

E. Ernst,[1] J. Reußner,[1] P. Poelt,[2] E. Ingolic[2]

[1]*Borealis GmbH, Linz, Austria*
[2]*Research Institute for Electron Microscopy, Graz University of Technology, Graz, Austria*

Received 21 July 2003; accepted 22 November 2004
DOI 10.1002/app.21743
Published online in Wiley InterScience (www.interscience.wiley.com).

ABSTRACT: Thermoplastic olefins based on polypropylene compounds are being increasingly used for the production of painted automotive parts. The poor adhesion properties of these compounds are improved with flaming, which results in good adhesion for waterborne paints. The surface stability and adhesion properties of two commercial injection-molded compounds and their base polymer blends (polypropylene/ethylene–propylene rubber) were investigated after they were flamed with various parameters under typical vapor jet conditions. The compounds and the corresponding base blends showed mainly the same behavior. Thus, filler particles and additives seemed to have only a minor influence on the adhesion properties of these compounds. For the characterization of the surface itself and the near-surface region, scanning and transmission electron microscopy, XPS, and microthermal analysis were used. The utmost surface layer for all specimens consisted of a skin of pure polypropylene. The oxygen concentrations at the surface after flaming were rather similar for both compounds. Differences could be found in the surface roughness, the oxygen diffusion from the interior to the surface, and, probably most importantly, the viscosity and elasticity of the impact modifier. © 2005 Wiley Periodicals, Inc. J Appl Polym Sci 97: 797–805, 2005

Key words: adhesion; electron microscopy; poly(propylene) (PP)

INTRODUCTION

Thermoplastic olefins (TPOs) are very important for the production of exterior automotive parts. Polypropylene (PP)/ethylene–propylene rubber (EPR) reactor blends are often used as base polymers because of their excellent cost–performance ratio. The final TPOs typically contain an additional external rubber, such as EPR, inorganic fillers such as talc, and various additives.

The decorative painting of bumpers, side trims, and panels is desired for esthetic reasons. To avoid environmental pollution, conventional solvent-borne paint systems are being replaced by waterborne ones. The painting of TPOs is a very complex process. The kind of paint used, the painting technology, the material composition, and the molding conditions of the TPO have a strong impact on paint adhesion, which is the key problem. Many of the correlations between the different parameters are not very well understood. Therefore, more data about the impact of the various process parameters on paint adhesion are needed.

Various results have been published about the adhesion and action mode of chlorinated polyolefin (CPO) containing primers[1,2] in lacquer systems. The diffusion of the CPO material into the topmost layer of the material with subsequent mechanical interlocking with cocrystallized PP has been discussed. For waterborne CPO-free basecoats, the adhesion mechanism should be much more complex.[3]

Both the composition of the TPO and the paint system and the surface morphology of the injection-molded materials have important effects on both the wettability of the TPO and the paint adhesion. The properties of the rubber phase seem to play an important role in the definition of the mechanical bulk properties and in the development of the surface morphology and the adhesion properties. During injection molding, a skin layer similar to the one observed in propylene homopolymers is formed. It does not contain rubber particles.[4,5] Tomasetti et al.[6] characterized the surface composition of PP/EPR blends: surface phase segregation should lead to the presence of mainly pure PP in the first 100 nm of the surface, but this PP skin should not be completely closed. The role of EPR in the formation of the skin layer is still speculative.

Ryntz[7] pointed out that rubber, which lies in a layer directly beneath the PP surface, is responsible for the paintability of TPOs. A mechanism for cohesive delamination of the substrate based on surface morphology as a function of the painting conditions has been discussed.

Correspondence to: P. Poelt (peter.poelt@felmi-zfe.at).

Journal of Applied Polymer Science, Vol. 97, 797–805 (2005)

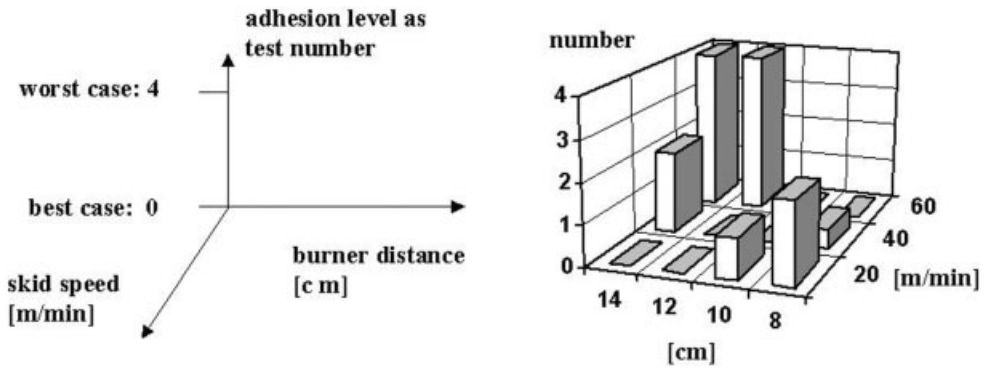

Figure 1 Characteristics of an adhesion diagram.

A general improvement in the adhesion level can be achieved by a surface pretreatment. The most important method from an industrial point of view is flaming. The effectiveness of the surface activation depends on process conditions such as the gas composition, burner distance, and residence time.[8,9] Simple methods such as vapor tests are often used for adhesion assessment in the automotive industry. Every car producer uses his own standards, which depend on different quality requirements.[10] From a practical point of view, high-pressure cleaners are used for car cleaning and deslushing. For the investigation of the wettability and adhesion on PP surfaces, plasma treatments have also often been used.[11–14]

The objective of this article is to improve the understanding of the correlation between the TPO composition, the surface morphology of injection-molded products, and the paint adhesion of waterborne paint systems. In particular, the influence of EPR is elucidated. Emphasis is also placed on industrial vapor jet tests for adhesion characterization.

EXPERIMENTAL

Materials

The materials were prepared on a Prism 24 twin-screw extruder (Prism Ltd., Staffordshire, UK). The maximum temperature of the melt was set to 240°C. The following conditions for the injection molding of test panels (80 mm × 150 × 2 mm) were used: melt temperature = 240°C, mold temperature = 50°C, and melt flow = 16 cm^3/s.

The standard laboratory painting process was composed of three consecutive steps. The panels were first purified in a simulated power wash process (pH 10, 45 bar, and 30°C). After being washed with desalinated water, the panels were dried at room temperature.

Flaming and painting

A burner by Herbert Arnold GmbH (Arnold Co., Germany), with propane as the burner gas was used for the activation of the panel surface. A propane/air ratio of 25 was adjusted for the flame pretreatment. To consider different flaming conditions, we varied the burner distance and skid speed (residence time of the flame).

A three-component metallic paint system (Herberts Co., Cologne, Germany) was applied for painting. A waterborne two-component polyurethane system (Cologne, Germany) was used as the basecoat with a thickness of 12 μm.

Adhesion tests

For the adhesion characterization, a vapor jet test was carried out. A stream of hot water with temperature T was directed for time t at distance d under angle α to the surface of the test panel, which contained a crosscut in the form of a St. Andreas cross. Pressure p was determined by the type of nozzle installed at the end of the water pipe. Different vapor jet test conditions are specified for the automobile industry.[6] The following conditions were used in this study: T = 60°C, t = 60 s, d = 100 mm, α = 90°, p = 68 bar, and nozzle type = 2506. The adhesion level was assessed by a number between 0 (no damage to the coating) and 4 (a large area of destruction of the lacquer layer). A comparison with standard specimens was used for the determination of these numbers.

A diagram was produced that described the paint adhesion with respect to the flaming conditions. The x axis indicated the burner distance (8–14 cm), the y axis showed the burner speed (20–60 m/min), and the z value was the corresponding adhesion level. Every peak represented adhesion failure. The principles of the activation–adhesion diagram are summarized in Figure 1.

XPS measurements

XPS measurements were performed with an SSX-100 spectrometer (Surface Science Instruments, Mountain View, CA) equipped with an Al Kα (1486.8 eV) source

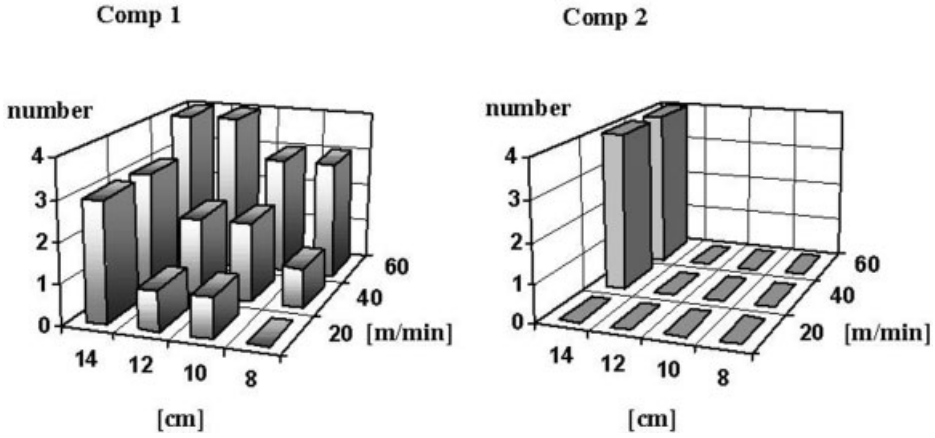

Figure 2 Paint adhesion for compounds 1 and 2.

used at 10.0 kV. The pressure in the analysis chamber was 10^{-9} mbar during data acquisition. The takeoff angle was 35° with respect to the sample surface, and it corresponded to an effective sampling depth of 5.7 nm.

Microthermal analysis

Microthermal analysis is based on the connection of scanning probe microscopy with the characterization capabilities of thermal analysis [thermomechanical analysis (TMA) and dynamic mechanical thermal analysis (DMTA)]. A small resistant heated wire loop is mounted at the end of a cantilever arm of the microscope. It scans the surface of a solid material to measure the topography in an area that is up to 100 μm $\times$ 100 μm. In addition, the probe can be held at a constant temperature. A thermal response signal is used to construct an image of the surface that is based on variations in the specimen's local thermal conductivity. The images are then used to select specific areas for a local thermal analysis. This measurement enables the determination of the softening behavior. The instrument used for this work was a model 2990 microthermal analyzer from TA Instruments (Alzenau, Germany); it was based on a TopoMetrix Explorer TMX2100 scanning probe microscope (TopoMetrix Corporation, Santa Clara, CA).

For the characterization of the surface, the specimens were mounted horizontally on the microscope stage. All topographical and heat conductivity measurements were performed with the force feedback mode. The following conditions were selected: force for cantilever contact = 3–4 nN/nA, cantilever tip (CT) response = 10 kHz, constant temperature for the tip = 50°C, modulation amplitude = 3°C, and frequency = 4 kHz. The scanning rate was varied between 50 and 200 μm/s and depended on the sample quality. For the thermal analysis the tip was calibrated by use of a certified polyamide 6.0 standard (202°C). The heating rate for the TMA measurements amounted to 5°C/s.

Etching

Chemical etching was performed in *n*-hexane at 60°C for 20 min.[15] The EPR phase was etched much more strongly than the PP matrix and thus removed, but only in those cases in which the particles had direct contact with the surface.

Oxygen etching was performed in a GEA 005 (ZFE Graz, Graz, Austria) at a pressure of 6×10^{-4} mbar.

Scanning electron microscopy (SEM)/energy-dispersive X-ray spectrometry instrumentation

The SEM images and the chemical analyses were recorded and processed with a Noran Voyager energy-dispersive X-ray spectrometer (ThermoNoran, Middleton, WI) and image processing system attached to a Zeiss DSM 982 Gemini field emission scanning electron microscope (Carl Zeiss SMT AG, Oberkochen, Germany). The electron energy (E_0) for SEM varied between 0.2 and 30 keV. At an electron energy of 5 keV, the penetration depth of the electrons in the specimen was approximately 1 μm (density (ρ) $\sim$ 1 g/cm^3). The image resolution was 1024 pixels $\times$ 1024 pixels.

Transmission electron microscopy (TEM) pictures were recorded with a Philips 300 and subsequently digitized.

RESULTS AND DISCUSSION

Paint adhesion and oxygen surface concentration

PP compounds for automotive applications have to fulfill various requirements with respect to the mechanical properties and applications. Therefore, they differ in their general compositions, including the filler and rubber concentrations. In Figure 2, the paint adhesion properties of two model compounds (compounds 1 and 2) used for bumpers are compared.

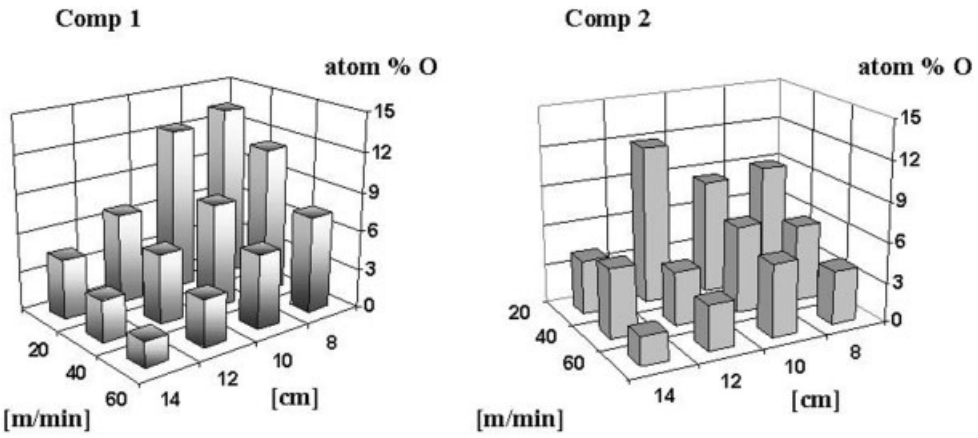

Figure 3 Surface concentration of oxygen for compounds 1 and 2, as measured by XPS.

Both materials consisted of PP/EPR reactor blends with an EPR concentration of 30 wt % and a talc concentration of 10 wt %. They mainly differed in the concentration of the additional external rubber; it was medium for compound 1 and high for compound 2. As a result, the Charpy notched impact strength was 35 for compound 1 and 60 for compound 2. The second important difference was the molecular weight of the external rubber. The intrinsic viscosity was low for compound 1 and high for compound 2.

Paint adhesion depends to a large extent on the activation of the surface by a flame pretreatment. Therefore, the oxygen concentrations of both compounds were determined by XPS with respect to the flaming conditions [skid speed (m/min) and burner distance (cm)]. The results are shown in Figure 3.

The surface oxygen concentration was on average higher for compound 1 than for compound 2. The difference can be partly explained by the higher additive concentration in compound 1. Pijpers and Meier[9] mentioned that certain additives in PP could cause unexpected adhesion problems. In addition, an increase in single peak heights was caused by filler particles, which were located in the scanned surface area of the XPS measurement. However, the differences in the oxygen concentrations were not substantial, and so the observed differences in paint adhesion could not be related to differences in the surface activation. Therefore, the influence of the single compound ingredients on the paintability was investigated in detail. The first target was the assessment of the influence of the base polymers used for the production of the compound.

Influence of the PP/EPR reactor blend composition on paint adhesion

PP/EPR reactor blends 1 and 2 were injection-molded and painted in the same way described for compounds 1 and 2. The results of the vapor jet tests are presented in Figure 4.

The PP/EPR reactor blends showed nearly the same differences in paint adhesion as the final compounds (Fig. 4). A correlation between the adhesion level and

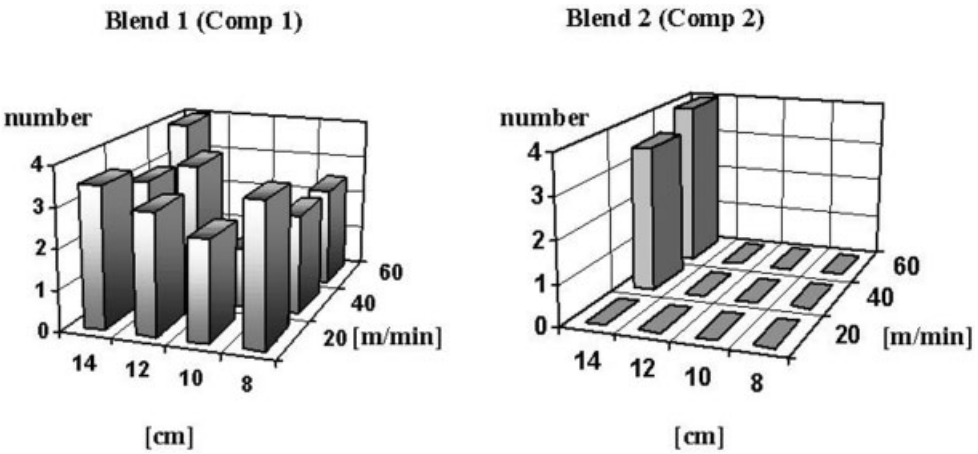

Figure 4 Results of the vapor jet test with respect to the flaming conditions for blends 1 and 2.

TABLE I
Composition and Properties of PP/EPR Blend 1 and Blend 2

Property	Blend 1	Blend 2
MFR_{blend} (g/10 min)	12	6
MFR_{matrix} (g/10 min)	40	40
EPR content (wt %)	30	30
IV_{XCS} (dL/g)	Low	High
C_2 content (mol %)	Medium	Medium

MFR = melt flow rate (a higher melt flow rate corresponded to a higher viscosity); IV_{XCS} = intrinsic viscosity of the xylene-soluble fraction (rubber phase).

Vicat A temperature as a measure of the surface stability was not found. The general adhesion level apparently was strongly dependent on the composition of the pure PP/EPR reactor blends. The compositions of the materials depicted in Figure 4 are summarized in Table I.

The matrix melt flow rate was the same for blends 1 and 2. The two blends differed only in the molecular weight of EPR. The influence of EPR on the paint adhesion was analyzed for these blends, and the surface compositions of the different PP materials were determined by several methods (SEM, TEM, and microthermal analysis).

Surface structure and composition of PP compounds based on PP/EPR reactor blends

SEM/EDX

In a first approach, we tried to image the surfaces and to analyze the phase compositions of both the panel surface and the core material by SEM. In general, the rubber phase can be etched by *n*-hexane, and the distribution and geometry of the holes gives the distribution and geometry of the particles of the EPR phase. The surfaces of the injection-molded panels before and after flaming appeared chemically inert. As Figure 5 demonstrates, no changes were visible after edging with hexane. However, in the cross sections the rubber phase could be extracted without any problem. Thus, there was a significant difference in the compositions of the surface and the core material. Because of the excellent wettability of the EPR particles by PP, these particles did not form part of the actual specimen surface. The surface was made up of a skin of pure PP after both injection molding and flaming. This phenomenon is often emphasized for PP/EPR blends.[5] The reasons may be the different melting points and viscosities of the two phases. Flaming does not have the effect of removing this skin and making the EPR phase directly accessible from the surface.

A clear difference could be observed in the structures of the surfaces of reactor blends 1 and 2 and their modified versions, compound 1 (blend 1) and compound 2 (blend 2). The surface of compound 1 was much smoother, most likely because of the lower molecular weight of EPR. The surface structure did not change substantially with flaming (Fig. 6; cf. also Fig. 5). Therefore, we should question whether the much rougher and irregular surface of the compound 2 specimens was not one of the reasons for the much higher resistance to break-away of the paint during the adhesion test with the water vapor jet.

Novák and Florián[16] showed that the adhesion properties of such systems strongly deteriorate with increasing concentrations of inorganic filler particles. Figures 2 and 4 show just the opposite effect. However, we should consider that the filler concentrations of compounds 1 and 2 were rather small. Although there was little influence of the filler on the compound 2/blend 2 system, the base material blend 1 showed a worsening in the results of the adhesion test in comparison with those of compound 1 (cf. Figs. 2 and 4).

In the next approach, we tried to remove the obviously existing PP skin layer by ion etching.[17] The samples were treated with oxygen plasma. Similarly

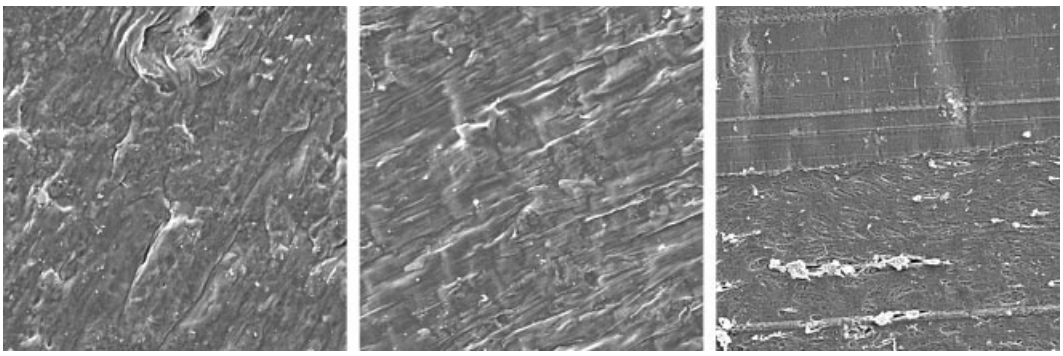

Figure 5 SEM images of compound 2, showing, from left to right, the surface of the untreated sample, the surface of the flamed sample, and the cross section of the untreated sample embedded in the resin (the resin is shown in the upper half of the image). All samples were *n*-hexane-edged (E_0 = 5 keV, image width = 57.3 μm).

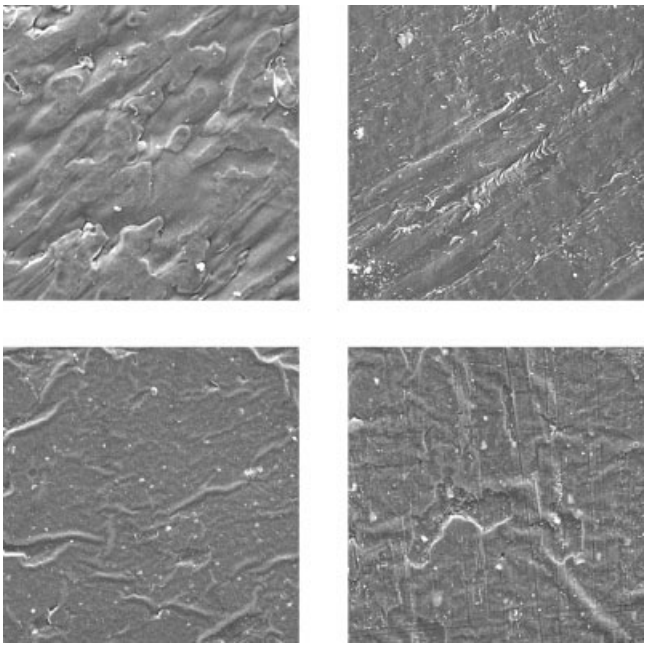

Figure 6 SEM images, clockwise from the upper left, of the surface of blend 2, the surface of blend 1, the surface of flamed compound 1, and the surface of compound 1 (E_0 = 5 keV, image width = 57.3 μm).

to flaming, it was not possible to remove the skin layer completely, even after a long-term treatment of 10 min. This result was not unexpected because both flaming and oxygen etching caused melting and burning of the surface. However, the removal of the skin layer could be clearly observed for the filler particles in the modified grades after longer etching times (Fig. 7). Under the assumption that the skin layers on the filler and EPR particles were approximately equal in thickness, the skin layer thickness should have been substantially lower than 0.5 μm.

Figure 7 demonstrates that after the etching process, freestanding uncoated filler particles remained at the surface. Thus, the wettability of these filler particles by PP was rather poor in comparison with that of the EPR particles. This could be at least a partial reason for the

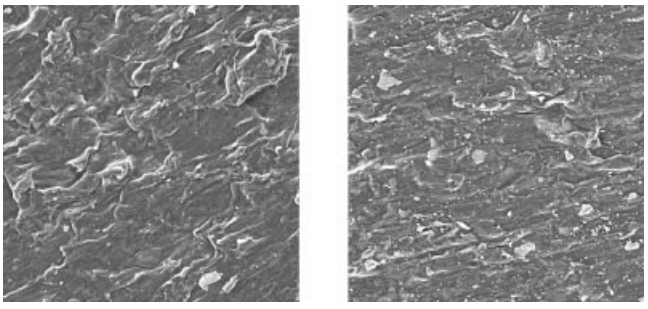

Figure 7 SEM images of compound 2, showing the untreated surface on the left and the ion-etched surface (O_2, 6 min) on the right (E_0 = 5 keV, image width = 57.3 μm).

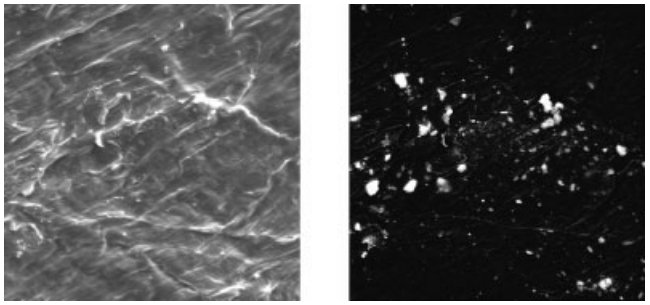

Figure 8 SEM images of compound 2, showing the surface on the left and the distribution of filler particles (bright spots and areas) close to the surface in the same area on the right (E_0 = 5 keV, image width = 57.3 μm).

dependence of the adhesion properties on the flaming parameters, especially when the agglomeration of filler particles close to the surface did take place (Fig. 8).

There was an additional difference between compounds 1 and 2. Compound 1 contained a higher concentration of oxygen-rich additives. For the irradiation of the surface of compound 1 during SEM with high probe currents, the diffusion of oxygen or oxy-

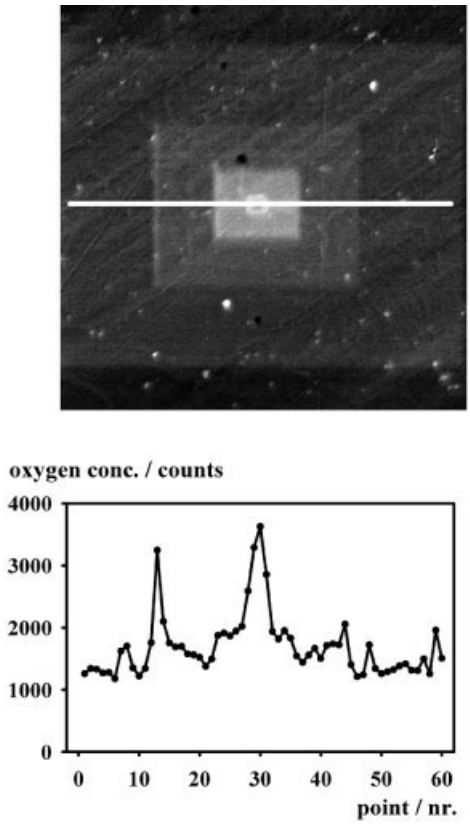

Figure 9 SEM image of compound 2 (E_0 = 5 keV, image width = 114.7 μm) with an oxygen line scan along the white line after the irradiation of the sample surface at different magnifications (visible as areas of different brightness; higher brightness means longer irradiation) for several minutes (E_0 = 5 keV, probe current (I) ~ 1.5 nA).

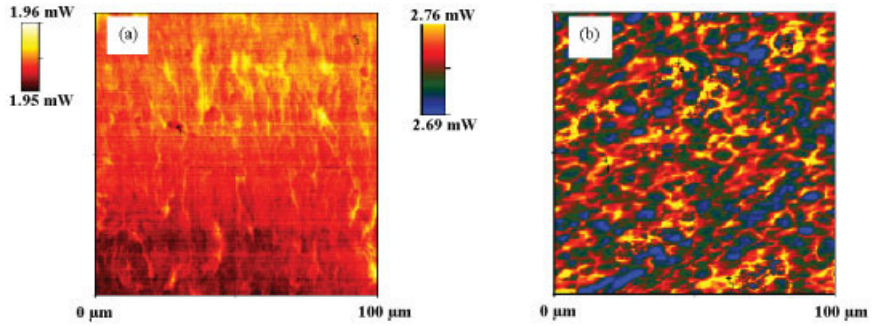

Figure 10 Thermal conductivity images of injection-molded panels of compound 2 (a) on the surface and (b) in the bulk.

gen-rich molecules to the irradiated surface could be observed (Fig. 9). Because during SEM the specimen was *in vacuo* (better than 10^{-6} Torr), the only source of oxygen was the specimen itself. Because the main reason for oxygen diffusion was the heating of the specimen, it could also occur with flaming or plasma treatment. However, the diffusion of oxygen from the specimen interior to the surface changed the oxygen concentration on the surface, and nonpolar additive parts could possibly have covered polar groups. The results in this case also strongly depended on the flaming conditions. A detailed discussion of the surface changes of polyethylene and PP by flaming can be found in ref. 18.

Brun et al.[19] found that the chemical modifications produced by the irradiation of PP by α particles were dependent on the atmosphere during the irradiation. This supports the idea that for flaming adhesion is dependent on the gas composition. Studies of the natural aging of PP have additionally proved that chemical modifications are also induced by simultaneous exposure to light.[20]

An investigation of the failures caused by peel forces demonstrated that all the failures could be located in the substrate at some depth below the modified surface layer. Thus, the degree of modification of the surface did not directly determine the degree of paint adhesion. Nihlstrand et al.[12] argued that paint adhesion properties are strongly influenced by the extent of chain-scission reactions in the near-surface region of the substrate during flaming or plasma treatment.

Microthermal analysis

In a second series of investigations, the surfaces and cross sections of injection-molded panels consisting of PP/EPR blends were investigated with microthermal analysis. Typical conductivity pictures and softening curves of the surface and cross section of compound 2 panels are depicted in Figures 10 and 11. In Figure 10, a colored scale is given on the left side of each picture. It indicates the difference in the thermal conductivity (mW). The differences in color are proportional to those in thermal conductivity.

The variations of the thermal conductivity at the surface of sample compound 2 were nearly negligible. As a result, the surface layer of the test panel was very homogeneous. Inside the material, larger differences could be detected. The compositions of the phases involved in the formation of the material could be characterized by their softening behavior. On the surface of the panel, only one type of softening curve could be observed [Fig. 11(a)], and this is typical for PP homopolymers. At the cross section, all three phases—PP, EPR, and inorganic filler particles—were detectable. The matrix polymer was represented by the same curve representing the surface. The sensor

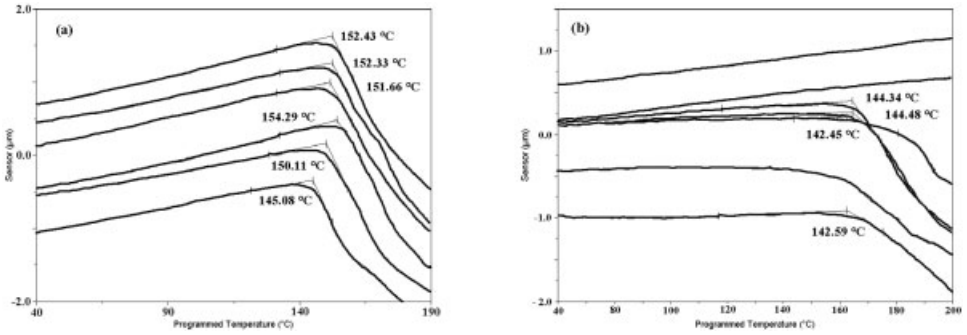

Figure 11 Softening curves measured (a) on the surface and (b) in the bulk of compound 2 panels.

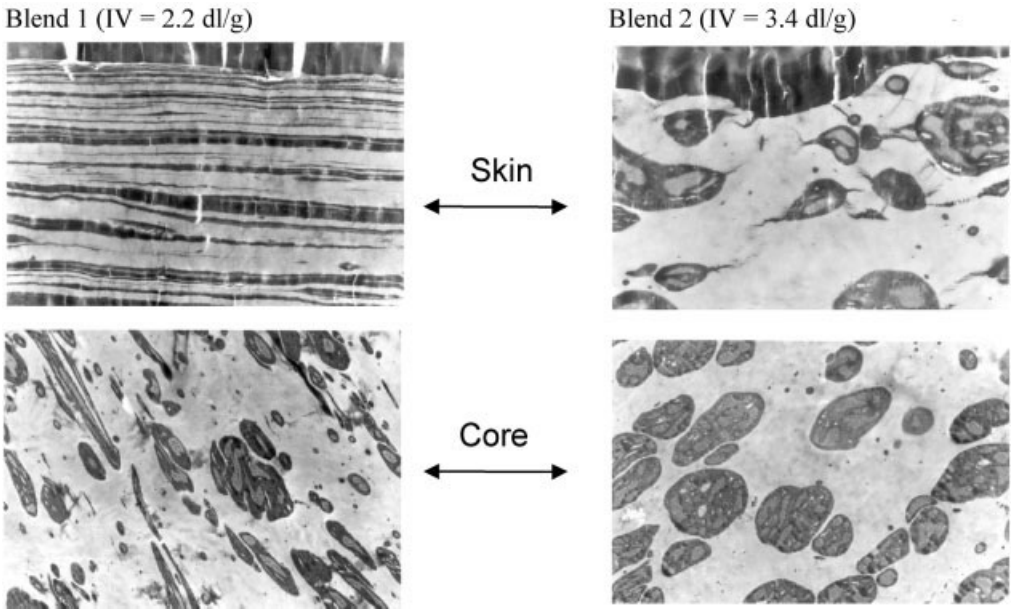

Figure 12 TEM images of the skin–core morphology of PP/EPR blends with different EPR viscosities (the specimen boundary is close to the upper image boundary; image width of top images = 6.5 μm, image width of bottom images = 17.9 μm).

tip penetrated the surface for the rubber particles or had no deflection for the filler particles [see the two uppermost curves in Fig. 11(b)].

The softening range of the PP matrix was investigated in the next step for blends 1 and 2 and corresponding compounds 1 and 2. This was done with respect to speculations about the influence of low-molecular-weight EPR fractions on the surface composition and surface stability in the last section. The results are summarized in Table II.

The surfaces of all the materials in Table II correspond to the PP homopolymer. Only one type of softening curve could be detected. The softening temperature for the homopolymer was 150°C on the surface and in the bulk. Nearly the same values were found for blend 2. The softening temperature of blend 1 was 6–7°C lower than that of blend 2. The softening behavior reflected the crystallization behavior inside the PP skin layer. The low-molecular-weight fraction (xylene cold solubles (XCS) fraction) was soluble in the amorphous regions of PP. Cocrystallization with the PP matrix during injection molding took place.[21] The smaller crystallites had a reduced melting point, and this caused the decrease in softening.

TABLE II
Softening Behavior of PP/EPR Blend 1 and Blend 2 and Their Corresponding Compounds

Material	IV_{XCS} (dL/g)	T_{soft} surface (°C)	T_{soft} bulk (°C)
PP homopolymer	—	150	150
Blend 1	Low	145	144
Blend 2	High	151	149
Compound 1	Low	143	144
Compound 2	High (< blend 2)	150	143

IV_{XCS} = intrinsic viscosity of the xylene-soluble fraction (rubber phase); T_{soft} = softening temperature.

For the compounds, the same tendencies were found, with the exception that the bulk value for compound 2 was lowered too. One reason could be the use of an external rubber, the molecular weight of which was not as high as that of EPR in blend 2. The low molecular fraction of the external rubber could cause the reduced softening temperature by the same mechanism discussed previously.

TEM investigations

According to the results presented in the literature, different viscosity ratios should have a significant impact on the surface morphology and stability.[5] Therefore, the distribution of the rubber particles was characterized by TEM with respect to their viscosity and position in the skin and bulk of the injection-molded panels (Fig. 12).

In blend 2, compact rubber particles could be observed in the core material. In the region of the skin layer, the same particles with low elongations were visible. The skin layer was not disturbed and covered the rubber particles. For blend 1 with the lower viscosity, the rubber particles were much more elongated even in the core of the panel. In the skin area, the particles had a laminar structure.

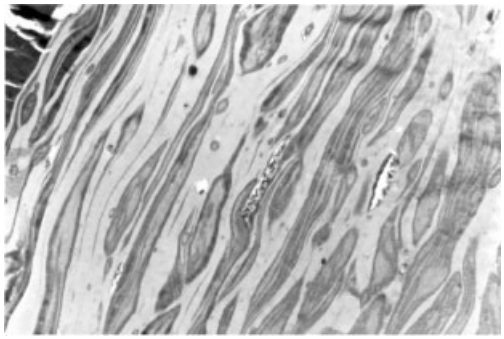

Figure 13 TEM image of the near-surface morphology of compound 2 (image width = 17.9 μm).

To adjust the final compound properties, such as the impact strength or elongation at break, additional external rubber was necessary. When the viscosity of the additional rubber was lower than that of EPR, the overall rubber viscosity was also reduced. One result was the reduction of the softening temperature, as discussed previously. The second result was the elongation of the rubber particles close to the surface. An example is given in Figure 13 for final compound 2. The surface is in the upper left corner.

A low-viscosity and low-elasticity impact modifier reduces surface stability and may cause delamination. With respect to the paint adhesion results for the different PP/EPR blends during vapor jet testing, an important reason for the observed differences is obvious. When hard conditions (high pressure) are applied, the adhesion level can be characterized only for materials for which the rubber viscosity and surface stability are high enough to withstand the delamination. For low-viscosity material blend 1, the delamination process hid the adhesion effect. The surface stability of the PP/EPR blends determined the stability of the final compounds to a large extent.

CONCLUSIONS

Two commercial injection-molded compounds and their base polymers were subjected to the vapor jet test method. The results for the compounds and their corresponding base polymers were very similar; for example, filler concentrations up to 10% had no significant influence on paint adhesion. However, the two compounds showed very different behaviors for paint adhesion.

As was proven by several methods, the utmost surface layer consisted in both cases of a skin of pure PP. Differences could be found in

1. The surface structure and roughness.
2. The diffusion of oxygen from the specimen interior to the surface, which resulted from different amounts of oxygen-containing additives.
3. The viscosity and elasticity of the impact modifier, which for these specimens was probably the most important factor for paint adhesion.

Additionally, the vapor jet test method proved to be a very useful tool for the study of the surface stability of the PP compounds.

The authors thank K. Peter (Deutsches Wollforschungsinstitut Aachen) for the X-ray photoelectron spectroscopy measurements.

References

1. Clemens, J. C.; Batts, G. N.; Lawniczak, J. E.; Middleton, K. P.; Sass, C. Prog Org Coat 1994, 24, 43.
2. Prater, T. J.; Kaberline, S. L.; Holubka, J. W.; Ryntz, R. A. J Coat Technol 1996, 68, 83.
3. Grundke, K.; Jacobasch, H.-J. Farbe Lack 1992, 98, 943.
4. Fujiyama, M.; Awaya, H.; Kimura, S. J Appl Polym Sci 1977, 21, 3291.
5. Karger-Kocsis, J.; Csikai, I. Polym Eng Sci 1987, 27, 241.
6. Tomasetti, E.; Nysten, B.; Rouxhet, P. G.; Poleunis, C.; Bertrand, P.; Legras, R. Surf Interface Anal 1999, 27, 735.
7. Ryntz, R. A. Prog Org Coat 1996, 27, 241.
8. Gerbassi, F.; Morra, M.; Occhiello, E. Polymer Surfaces from Physics to Technology; Wiley: New York, 1994; Chapter 6.
9. Pijpers, A. P.; Meier, R. J. J Electron Spectrosc Relat Phenom 2001, 121, 299.
10. Thomas, G. Kunststoffe 1990, 80, 24.
11. Nihlstrand, A.; Hjertberg, T.; Johansson, K. Polymer 1997, 38, 3581.
12. Nihlstrand, A.; Hjertberg, T.; Johansson, K. Polymer 1997, 38, 3591.
13. Carrino, L.; Moroni, G.; Polina, W. J Mater Process Technol 2002, 121, 373.
14. Morra, M.; Occhiello, E.; Gila, L.; Garbassi, F. J Adhes 1990, 33, 77.
15. Mirabella, F. M. J Polym Sci Part B: Polym Phys 1994, 32, 1205.
16. Novák, I.; Florián, Š. J Mater Sci Lett 1994, 13, 1211.
17. Chan, C.-M. Polymer Surface Modification and Characterisation, Plasma Modification; Hanser: Munich, Germany, 1994; Chap. 6.
18. Papirer, E.; Wu, D. Y.; Schultz, J. J Adhes Sci Technol 1993, 7, 343.
19. Brun, C.; Chanbaudet, A.; Mavon, C.; Berger, F.; Fromm, M.; Jaffiol, F. Appl Surf Sci 2000, 157, 85.
20. Rjeb, A.; Letarte, S.; Tajounte, L.; Chafik, E. I. M.; Adnot, A.; Roy, D.; Claire, Y.; Kaloustian, J. J Electron Spectrosc Relat Phenom 2000, 107, 221.
21. Ryntz, R. A.; McNeight, A.; Ford, A. Plast Eng 1996, 52, 35.